

# Processing and characterization of thermoplastic starch/polycaprolactone/compatibilizer ternary blends for packaging applications

M. P. Guarás<sup>1</sup> · V. A. Alvarez<sup>1</sup> · L. N. Ludueña<sup>1</sup>

Received: 29 May 2015 / Accepted: 27 July 2015  
© Springer Science+Business Media Dordrecht 2015

**Abstract** Thermoplastic starch (TPS)/polycaprolactone (PCL) blends were obtained by melt mixing. First, the best formulation of thermoplastic starch (starch, plasticizer and additives) was studied. The obtained films were characterized by means of differential scanning calorimetry, DSC (melting temperature and crystallinity degree); thermogravimetric analysis, TGA (real composition of the blend and thermal stability); tensile tests (mechanical properties); infrared spectroscopy, FTIR (interactions between components); scanning electron microscopy, SEM (morphology); and water absorption tests. The effect of PCL/TPS ratio on the previously mentioned characteristics and properties were studied. In addition, the effect of using PCL modified with maleic anhydride as compatibilizer was also analyzed. An optimal compatibilizer content was found improving the mechanical properties and slowing down the degradation rate in soil of the blends. On the other hand, a slight increase in the water absorption of the blends was found in comparison with the non-compatible ones.

**Keywords** Thermoplastic starch · Polycaprolactone · Grafting · Mechanical properties · Biodegradability

## Introduction

It is known that waste accumulation is actually a serious problem and, so that, the development of environmental friendly, degradable, polymeric materials has attracted extensive interest [1, 2].

The non-biodegradability of most plastics has caused many environmental problems associated with their disposal. Not only are non-recyclable, but also cause problems in its post-consumer treatment because they are largely inert to microbial attack. This fact has carried to an increased interest in the use of biodegradable polymers [3].

In recent times, the development of starch-based products has a growing interest, since starch is a fully biodegradable and environmental friendly material [4]. Starch is an abundant and low cost natural biopolymer obtained from renewable resources. The starch grains consist in macromolecules arranged in layers. A mixture of two polysaccharides in different ratios, amylose (linear) and amylopectin (branched), composes starch [5]. This macromolecular structure is suitable for the production of bioplastics. However, prior to production of such materials, the structure of native starch should be suitable modified. This is necessary since starch degradation starts at a lower temperature than its melting point, and thus native starch cannot be processed by conventional plastics technology prior to any modification [6]. This modification is performed by the breakdown of the starch granule when it is processed in the presence of a specific amount of plasticizer, mainly s, at a given temperature [1]. The resulting material is called thermoplastic starch (TPS). Nevertheless, the TPS is a material which usually has low stability in high moisture conditions and has a fragile nature, assisted by eventual migration of plasticizers to the environment [7]. Blending TPS with other polymers has been commonly used. Bikiaris et al. [8], have developed blends with synthetic polymers such as

---

✉ L. N. Ludueña  
luduenanmdp@gmail.com

<sup>1</sup> National University of Mar del Plata (UNMDP), National Scientific and Technical Research Council (CONICET), Research Institute of Materials Science and Technology (INTEMA), Composite Materials Group (CoMP), Solís 7575, B7608FDQ Mar del Plata, Argentina

polyethylene leading to non-fully biodegradable materials. TPS is also blended with other biodegradable polymers such as aliphatic polyesters, i.e. polycaprolactone (PCL) [7], poly(hydroxyl butyrate) [9] and poly(lactic acid) [10], in order to improve their properties maintaining the biodegradation capacity of the material. Among them, PCL is a promising synthetic biodegradable material, because of its very high flexibility and its hydrophobic nature [11]. It is also one of the more commercially available biodegradable polymers. However, it is still expensive to be widely used as required by packaging applications. This is the reason why it is blended with lower-cost natural biopolymers such as thermoplastic starch.

The main issue to overcome in the preparation of TPS/PCL blends is the poor compatibility and weak adhesion between the polysaccharide and the synthetic polymer matrices owing to their different polarity giving consequently poor final properties [12]. In fact, starch and hydrophobic polymers (such as PCL) are immiscible and simple mixing lead to phase separated blends. In order to improve their compatibility, and so the adhesion between the two immiscible polymers, a reactive functional group (maleic anhydride) onto the PCL phase can be introduced to increase the polar nature of this polymer, consequently improving the adhesion between the components of the system [3, 12]. Blending of PCL and TPS, with a reactive functional group grafted onto PCL, offers the best balance between low cost and good mechanical properties [7].

The aim of this work was to optimize both, TPS and TPS/PCL formulations looking for the lowest water vapor adsorption and the strongest mechanical properties. In the case of TPS, the effect of plasticizer content was analyzed. Then, the composition of TPS, PCL and PCL modified with maleic anhydride (PCL-gAM) fully biodegradable ternary blends was optimized. The morphology, thermal and mechanical properties and biodegradability of the blends was studied.

## Experimental

### Materials

Cassava starch purchased from Almidonera Diesel Argentina was used in powder form. The plasticizer used was ethylene glycol (EG, JT Baker). Stearic acid was used (SA Shuchardt Merck OHG) as a lubricant for processing.

Polycaprolactone, having a molar mass of 80,000 g/mol, was supplied by Aldrich Chemistry.

Maleic anhydride (MA), from Carlo Erba Reagents product, was used to prepare the compatibilizer.

Benzoyl peroxide (BP) from Aldrich Chemistry was used as initiator of the grafting reaction.

### Preparation of thermoplastic starch

Cassava starch (CS) and plasticizer (ethylene glycol, EG) were pre-mixed in a beaker. A small amount of stearic acid (SA 0.5 wt.%) was added as a processing agent. The mixture was introduced in a Brabender type mixer. The first step consisted on looking for the minimal plasticizer content needed for the gelatinization of native starch avoiding thermal degradation. We also optimized temperature (T), screw rotation speed (SRS) and residence time (RT) in the mixer. We found optimal mixing conditions in the Brabender type mixer at 120 °C and 60 rpm for 6 min, respectively, for 25 wt.% of plasticizer. Lower T, SRS, RT, and/or plasticizer content were not enough for complete gelatinization. Higher values of T, SRS and/or RT induced TPS thermal degradation. On the other hand, we used plasticizer contents up to 35 wt.% because at higher contents the Young's modulus of the TPS was so low that samples for mechanical testing could not be prepared.

The effect of plasticizer content ranging from 25 to 35 wt.% on the TPS water absorption and mechanical properties was analyzed. Table 1 shows the composition of the samples.

### Preparation of the compatibilizer

The compatibilizer was prepared by blending 95/4.5/0.5 wt.% of PCL/AM/BP in a Brabender Type mixer at 110 °C and 60 rpm for 7 min. The composition and conditions were chosen looking for the highest anhydride content of the grafted polymer according to the work by John et al. [13]. The compatibilizer was named PCL-gAM.

### Preparation of the PCL/PCL-gAM/TPS ternary blends

The blends were prepared by intensive mixing in a Brabender type mixer at 110 °C and 60 rpm for 6 min. TPS25 was used because it showed the best mechanical properties and lower water absorption. The different contents of TPS25, PCL-gAM and neat PCL were added simultaneously into the mixer. Blends with several TPS25 contents (0, 25, 50 and 75 wt.%) were prepared. The PCL-gAM content (0, 5, 10 and 15 wt.%) was also varied for each TPS25 content. Then, films of 0.7 mm×15 mm×20 mm were obtained by compression molding in a hydraulic press by following the next program:

**Table 1** Composition of the thermoplastic starch

Sample	CS (wt.%)	EG (wt.%)	SA (wt.%)	EG/CS Ratio
TPS25	74.5	25	0.5	0.3
TPS30	69.5	30	0.5	0.4
TPS35	64.5	35	0.5	0.5

10 min at 120 °C and 0 kg/cm<sup>2</sup>, 10 min at 120 °C and 50 kg/cm<sup>2</sup> and finally mold cooling with water up to 30 °C. The films were identified by three numbers, X/Y/Z, where the first number corresponds to the wt.% of PCL, the second number to the wt.% of PCL-gAM and the last one to the wt.% of TPS25.

## Characterization

Water vapor absorption (WVA) experiments were conducted on 20 mm side square shape specimens. Prior to the water vapor absorption measurements, the samples were dried in a vacuum oven at 30–35 °C for 48 h. The samples were conditioned in hermetic containers at room temperature with 65 % of relative humidity (RH). This condition was achieved by using a solution of glycerin and water, according with the ASTM D5032. The amount of water vapor absorbed by the samples was calculated by weighing them periodically, until a constant weight was attained. The water vapor uptake (WVA) was given by the following equation:

$$WVA(\%) = \frac{M_t - M_0}{M_0} \times 100 \quad (1)$$

where  $M_t$  is the weight at time  $t$  and  $M_0$  the initial weight of the sample

Thermogravimetric tests (TGA) were carried out with a Shimadzu TGA-50. Samples were heated at a constant rate of 10 °C/min from room temperature to 700 °C, under nitrogen atmosphere. The temperatures for maximum degradation rates of TPS components were calculated from derivative thermogravimetric analysis (DTGA).

Thermal characterization was carried out by using a Q2000 TA Instrument differential scanning calorimeter (DSC). About 8 mg of the samples were weighed accurately into aluminum pans and sealed hermetically. The samples were cooled down to –80 °C, and then heated to 250 °C at a heating rate of 10 °C/min under nitrogen atmosphere. Finally they were cooled down to room temperature. The crystallinity degree of pure PCL and PCL in the blends was calculated by the following equation:

$$X_c(\%) = \frac{\Delta H_m}{w_{PCL} \times \Delta H_{100}} \times 100 \quad (2)$$

where  $\Delta H_m$  is the experimental heat of melting,  $w_{PCL}$  the PCL weight fraction and  $\Delta H_{100}$  is the heat of melting of 100 % crystalline PCL ( $\Delta H_{100}$  136.1 J/g [14]).

Infrared Spectroscopy (FTIR) spectra were recorded with Mattson Genesis II instrument for a frequency range between 4000 and 600 cm<sup>–1</sup>. An average of 32 scans at a resolution of 4 cm<sup>–1</sup> was conducted at room temperature.

SEM micrographs of the cryo-fractured surface of the samples were taken with a JEOL JSM-6460 LV instrument. The

samples were prepared by cutting 10 mm×20 mm rectangular specimens after their immersion in liquid air to avoid the plastic deformation of the observed surface. Finally they were immersed in HCl (1 M) and dried at 30 °C in an oven, in order to dissolve the thermoplastic starch and uncover the cavities in order to differentiate one phase from another (TPS25 from PCL).

Tensile tests were performed on an INSTRON 4467 machine using a load cell of 100 N and operating at a constant crosshead speed of 10 mm/min for the PCL and 1 mm/min for the PCL/PCL-gAM/TPS25 blends. These conditions were selected according to the ASTM D882-91 standard. Before mechanical measurements, the samples were conditioned in a chamber at 65 % of relative humidity for 48 h at room temperature. All samples were tested at the same storage time in order to avoid differences about aging or plasticizer release to the environment on the mechanical performance.

Biodegradability of the samples was studied by evaluating weight loss of blends as a function of time in a soil environment at room temperature. Samples of 15 mm×15 mm×0.7 mm were weighed and then buried in boxes with soil. Natural microflora present in soil (Pinocha type) was used as the biodegrading medium. Soil was maintained at approximately 50 % moisture by weight and samples were buried at a depth of 15 cm. The samples were dried before buried them in a vacuum oven for 24 h at room temperature. Then, once unearthed, the samples were weighted to measure the water absorption and after that were dried in a vacuum oven for 24 h at room temperature to measure the weight loss.

Comparative graphs were done that showed the residual mass of the samples, calculated as the weight of the degraded sample to a certain time divided by its initial weight:

$$\text{Residual mass } (\%) = \frac{\text{weight of the degraded sample at time } t}{\text{initial weight of the sample}} \times 100 \quad (3)$$

## Results and discussion

### Effect of plasticizer content on the preparation of thermoplastic starch films

The plasticizer content in the preparation of thermoplastic starch was optimized looking for complete gelatinization avoiding thermal degradation, low water vapor absorption and improved mechanical properties.

#### Water vapor absorption

The TPS usually has low stability in high moisture conditions. The stability can be improved by reducing the water vapor

absorption of the material [1]. The compatibility of TPS with non-polar polymers such as PCL is also enhanced by this effect [12]. Figure 1 shows the WVA values at 65 % RH of the TPS as a function of plasticizer content.

The WVA values of TPS are high because the water molecules can easily diffuse to H-bonds with OH-groups of glucosyl units along the polymer chains [15]. It can be seen that WVA increases as a function of plasticizer content for the tests at 65 % RH. The strong affinity of ethylene glycol and water induces hydrogen bonding leading to an increment in the WVA as a function of ethylene glycol content [15].

#### Thermogravimetical analysis (TGA)

Figure 2 shows the DTGA curves of native starch and TPS as a function of plasticizer content. The temperatures of maximum degradation rate of the components calculated from the derivative thermogravimetical analysis (DTGA) analysis are included in Fig. 2.

The water content calculated by TGA for Native Starch, TPS25, TPS30 and TPS35 was calculated as the weight loss at 140 °C resulting in  $11.0 \pm 0.2$ ,  $15.5 \pm 0.3$ ,  $24.2 \pm 0.3$ ,  $24.0 \pm 2.7$  wt.%, respectively. These values are in accordance with those reported by Soares et al. and et al. [16, 17]. In addition, the water content was higher as a function of plasticizer content, as was expected from the water vapor absorption results.

The thermal degradation of native starch and TPS followed the typical behavior reported by several authors [16, 18–20]. In the case of native starch, a three-step reaction is observed. The first step was between 25 and 140 °C, which corresponds to the water loss, the second between 260 and 330 °C to starch decomposition and the third between 500 and 600 °C to the oxidation of partially decomposed starch [18]. A

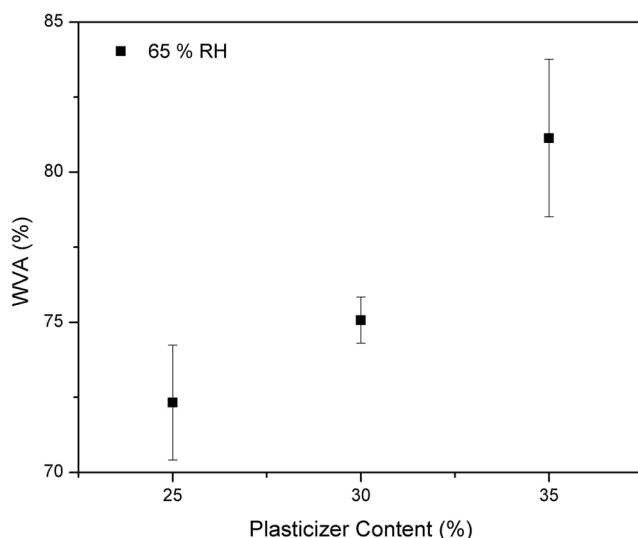


**Fig. 1** Water vapor absorption as a function of TPS plasticizer content

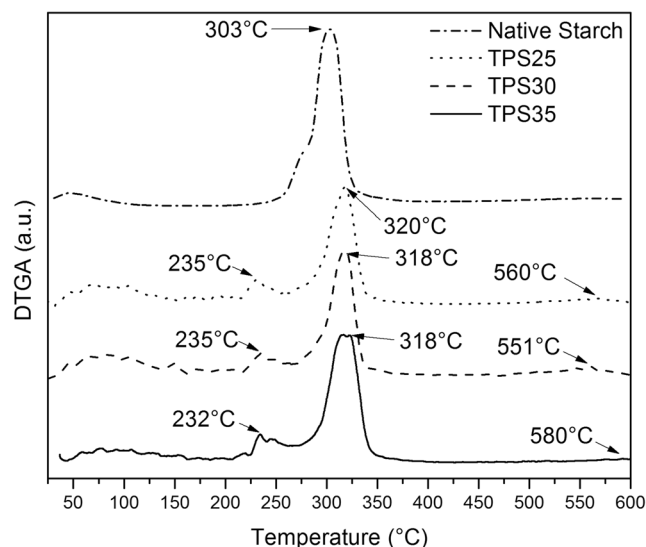


**Fig. 2** DTGA analysis of Native Starch and TPS with different plasticizer contents

shoulder is also observed in the range of 260 and 285 °C. The shoulder appears probably because the degradation events of the main peak occur through the series of competitive reactions, which includes depolymerization (which can be explained by the chain scission of the glycosidic linkage of polysaccharide), and subsequent decomposition of amylopectin and amylase products [19]. In the case of TPS, a fourth event between 210 and 250 °C is observed which corresponds to ethylene glycol degradation. The positions of the maximum of the TPS peaks were not significantly modified by changing the ethylene glycol content. It is concluded that the thermal stability of starch is not dependent of plasticizer content (in the range studied in this work).

#### Differential Scanning Calorimetry (DSC)

Figure 3 shows the DSC curves of TPS as a function of plasticizer content. The temperatures associated with the glass transition are also shown in Fig. 3.

The DSC curves present one change of heat capacity and an endothermic peak. The position of the endothermic peak at temperatures between 60 and 160 °C is attributed to water evaporation. The change of heat capacity observed at temperatures between -25 and 50 °C is slightly dependent on the amount of ethylene glycol: the higher it is, the lower the temperature of the heat capacity change. This decrease in temperature linked to heat-capacity change can be attributed to a glass transition temperature ( $T_g$ ) shift, due to increasing amounts of plasticizer. Moreover, the experimental values are in good agreement with the glass transition temperature reported in the literature [1, 15].



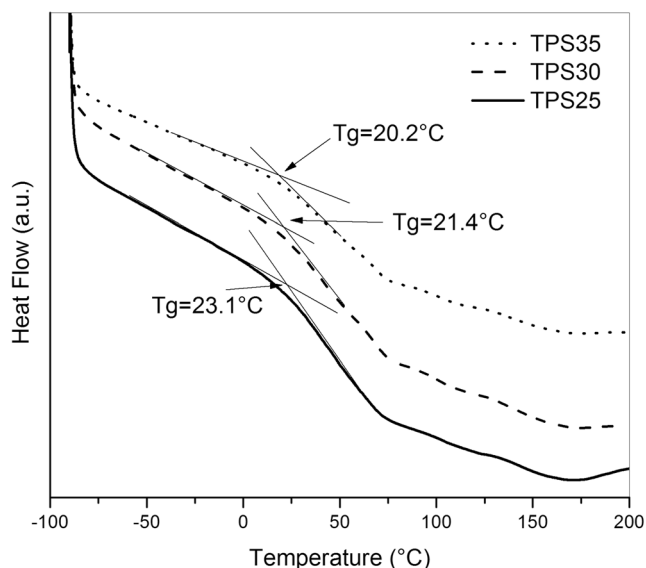


**Fig. 3** DSC curves of TPS as a function of plasticizer content

#### Fourier Transformed Infrared Spectroscopy (FTIR)

The microdomain structures of the native starch and TPS were analyzed by FTIR. The main bands for distinctive functional groups were identical in thermoplastic pure starch. Figure 4 shows the FTIR spectra of native starch, ethylene-glycol and TPS formulations.

The peaks corresponding to native starch and ethylene glycol are still present in all TPS formulations. In addition, the IR spectra of TPS were similar for all plasticizer contents. In the case of starch, the peaks at 1020 cm<sup>-1</sup> and 1075 cm<sup>-1</sup>–1150 cm<sup>-1</sup> were attributed to C–O stretching of C–O–C group

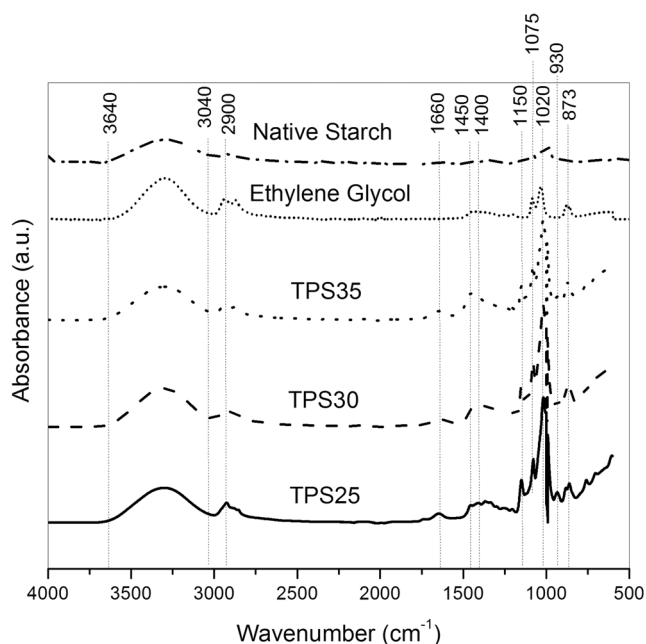


**Fig. 4** FTIR spectra of native starch and TPS with different plasticizer contents

in the anhydroglucose ring and C–O stretching of C–O–H group, respectively [21]. The wavenumbers in the range of 1400–1450 cm<sup>-1</sup> are assigned for O–H bonding. The peak position approximately at 1660 cm<sup>-1</sup> was due to the bound water present in the starch. The band at 2900 cm<sup>-1</sup> is associated with C–H stretching. A broad band due to hydrogen bonded hydroxyl group (O–H) appeared at 3040–3640 cm<sup>-1</sup> and is attributed to the complex vibrational stretching, associated with free, inter and intra molecular bound hydroxyl groups [22]. The bands corresponding to ethylene glycol are in similar positions than starch ones, so their disappearance or shifting are difficult to identify. Similar spectra for TPS as a function of plasticizer content suggests that the interaction between starch and plasticizer is physical but not chemical.

#### X-ray diffractometry (XRD)

X-ray diffraction technique is used to identify crystal structure and regular molecular arrangement presented in native and processed starches. Figure 5 shows the XRD spectra of native starch and TPS formulations.

Native cassava starch showed a typical A-type X-ray diffraction pattern, typical of cereal crystalline structure, with strong peaks at  $2\theta$  14.9°, 16.9° and 22.9° [5]. When extruded with plasticizer a significant reduction in crystallinity was observed and a transparent material was produced. During this process the starch granules are gelatinized and hence the glucosidic chains are retrograded into the V form. The retrograded TPS samples gives V-type diffraction pattern with the main peaks at  $2\theta$  13.1° and 20.0° [1]. Peaks near  $2\theta$  22.9° are still present in the TPS patterns, but their intensity is substantially reduced in comparison with native starch. In addition, the intensity of these peaks are reduced as a function of plasticizer content, indicating lower crystallinity. The

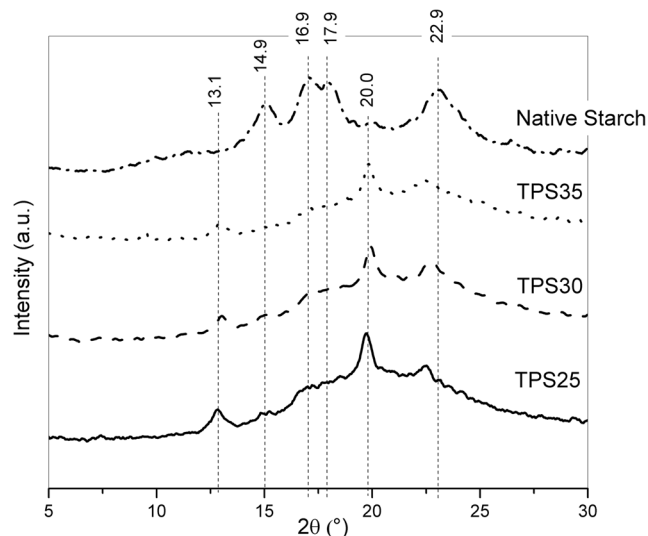


**Fig. 5** XRD spectra of native starch and TPS with different plasticizer contents

presence of these peaks indicates that some crystallinity still exists in the material. A fully amorphous material may be produced if the thermoplastic material was further processed or if higher plasticizer content would be used. Even so, significant deterioration/reduction of the molecular weight could take place with further processing, which might reduce the mechanical properties of the thermoplastic starch. On the other hand, plasticizer contents higher than 35 wt.% leads to a material so soft and fragile that it could not be mechanically tested.

### Mechanical properties

Table 2 shows the mechanical properties of TPS as a function of plasticizer content.

The Young's modulus and tensile strength decrease and the elongation at break increases as a function of plasticizer content. This behavior, including the reduction of glass transition temperature, is typical of plasticized green polymers [23–25].

TPS25 was the sample that showed the lowest water vapor absorption and the strongest mechanical properties. The chemical structure was not dependent on the plasticizer content. The TPS25 formulation was selected for the following studies.

### Characterization of PCL/PCL-gAM/TPS25 ternary blends

#### Water absorption

Figure 6 shows the equilibrium water uptake of the samples as a function of the content of compatibilizer and for the different amounts of TPS25.

Water absorption increased as a function of TPS25 content, due to the hydrophilic nature of this component. In most cases, at constant content of TPS25, the addition of compatibilizer did not produce a decrease in the water content of mixtures. By contrast, in the case of the mixture with 75 wt.% of TPS25 and 15 wt.% of PCL-gAM the absorption significantly decreased. These results demonstrated that there is not a clear relationship between the content of the compatibilizer and the water absorption of the samples. Bikiaris et al. [8] have found that this behavior can be attributed to the production of

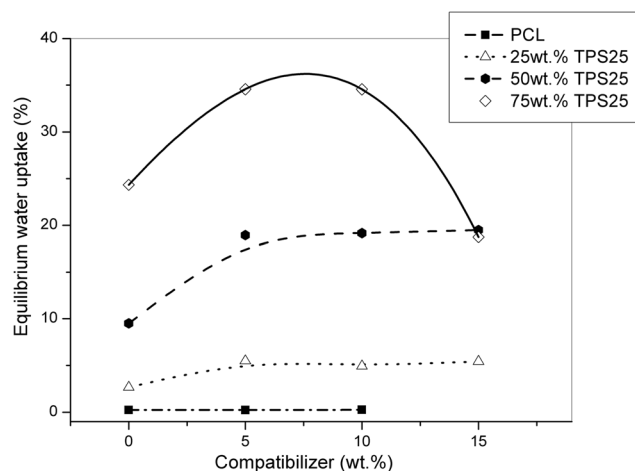


**Fig. 6** Equilibrium water uptake as a function of the content of compatibilizer

carboxylic groups which are hydrophilic in nature and, consequently, the compatibilized blends behaved more hydrophilically than the non compatibilized ones. On the other hand, Wu [3] have found the opposite result; they have shown that the reduction in water uptake in the presence of PCL-gAM is caused by the presence of ester carbonyl groups. This leads to a balance between available carbonyl groups and the amount of PCL and TPS25 in each material that determine the degree of water absorption of the final sample.

#### Thermal properties (DSC and TGA)

Figure 7 shows the DSC curves of the pure polymers and blends with 25 wt.% of TPS25 as a function of PCL-gAM content. Only blends with 25 wt.% of TPS25 were included because the curves of the blends with 50 wt.% and 75 wt.% of TPS25 showed the same shape. Table 3 resumes the thermal properties of the pure polymers and blends calculated by DSC.

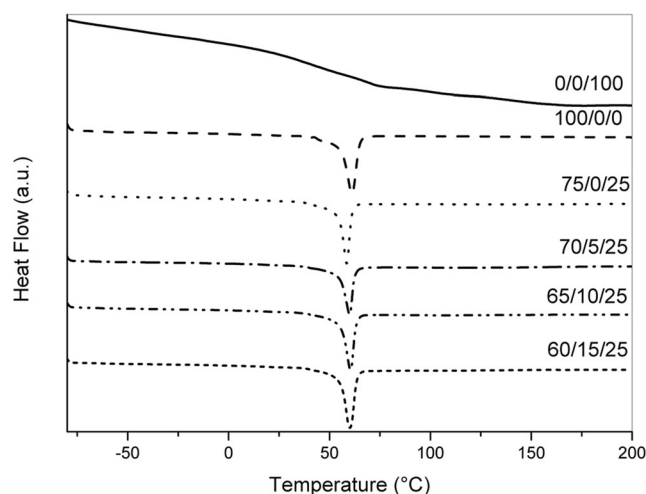


**Fig. 7** DSC curves of pure polymers and blends with 25 wt.% of TPS25 as a function of PCL-gAM content

**Table 2** Mechanical properties of TPS as a function of plasticizer content

Sample	Young's modulus (MPa)	Tensile Strength (MPa)	Elongation at break (%)
TPS25	27±20	1.0±0.1	23±1
TPS30	5±1	0.4±0.1	26±1
TPS35	2±1	0.2±0.1	28±1

**Table 3** Thermal properties of the pure polymers and blends calculated by DSC

Sample	T <sub>g</sub> <sup>a</sup> (°C)	T <sub>m</sub> <sup>b</sup> (°C)	ΔH <sub>m</sub> <sup>c</sup> (J/g)	X <sub>c</sub> <sup>d</sup> (%)	T <sub>1</sub> <sup>e</sup> (°C)	T <sub>2</sub> <sup>f</sup> (°C)	T <sub>3</sub> <sup>g</sup> (°C)	T <sub>4</sub> <sup>h</sup> (°C)
100/0/0	-61	61	74	54	—	—	—	402
95/5/0	-60	60	87	—	—	—	—	400
90/10/0	-60	61	87	—	—	—	—	400
85/15/0	-59	60	92	—	—	—	—	401
75/0/25	-58	59	63	62	—	305	—	401
50/0/50	-62	59	47	69	—	307	—	401
25/0/75	-57	58	22	65	—	305	—	401
70/5/25	-59	60	65	—	—	307	—	398
45/5/50	-61	59	50	—	—	306	—	397
20/5/75	-61	59	22	—	—	305	—	396
65/10/25	-60	60	66	—	—	303	—	396
40/10/50	-59	59	48	—	—	303	—	394
15/10/75	-63	58	26	—	—	303	—	394
60/15/25	-60	60	70	—	—	300	—	393
35/15/50	-62	59	49	—	—	300	—	392
10/15/75	-62	58	35	—	—	—	—	—
0/0/100	23	—	—	—	235	320	560	—

<sup>a</sup>T<sub>g</sub>=Glass transition temperature (DSC)<sup>b</sup>T<sub>m</sub>=Melting temperature (DSC)<sup>c</sup>ΔH<sub>m</sub>=Heat of melting (DSC)<sup>d</sup>X<sub>c</sub>=Crystallinity degree (DSC)<sup>e</sup>T<sub>1</sub>=EG decomposition (DTGA)<sup>f</sup>T<sub>2</sub>=Starch or TPS25 decomposition (DTGA)<sup>g</sup>T<sub>3</sub>=Starch oxidation (DTGA)<sup>h</sup>T<sub>4</sub>=PCL decomposition (DTGA)

The crystallinity degree of PCL slightly increased in the presence of TPS25. TPS25 could be acting as nucleation agent increasing the crystallization rate of the PCL phase. The crystallinity degree of the compatibilized blends could not be calculated because the ΔH<sub>100</sub> value of the PCL-gAM is not informed in the literature. On the other hand, the X<sub>c</sub> value of pure TPS25 could neither be calculated because the melting peak was superimposed with water evaporation and thermal degradation. For all samples, except to 0/0/100 corresponding to pure TPS25, an endothermic peak was observed around 56–60 °C. The enthalpy associated with this peak depends on the PCL content and allows us to attribute it to the melting of PCL. It was noticed that the melting temperature of PCL in the blend was only slightly depressed by the presence of TPS25. The blends with PCL-gAM showed almost the same melting point than the neat PCL, around 60 °C. Nevertheless, it was observed a slight increase of glass transition temperature which can be associated to the reduced segmental motion of random coil chains in amorphous regions and increased free volume through the presence in the end-chain of the encumbering molecules of maleic anhydride [12].

Figure 8(a,b) shows the TGA and DTGA curves of the pure polymers and blends with 25 wt.% of TPS25

as a function of PCL-gAM content. The curves of the blends with 50 wt.% and 75 wt.% of TPS25 showed the same shape.

The temperatures for the maximum degradation rates of the main events of all materials are resumed in Table 3. The maximum thermal degradation rate of pure PCL takes place at about 400 °C (T<sub>4</sub>). TPS25 showed two main peaks. The first one at one at 236 °C corresponding to ethylene glycol thermal degradation (T<sub>1</sub>) and the second one at 320 °C corresponding to starch decomposition (T<sub>2</sub>). The height of the peak corresponding to starch oxidation (T<sub>3</sub>) was significantly lower than that of starch decomposition (T<sub>2</sub>), so it cannot be seen in Fig. 8 due to the number of curves added in the same graph. The peak corresponding to ethylene glycol could not be seen in the curves of the blends with PCL because its height was significantly lower than that of the PCL (T<sub>4</sub>). In the case of the PCL/TPS25 blends, the presence of two degradation processes can be observed. The first one occurs between 270 °C and 350 °C, and corresponds to the TPS25 phase (EG and starch decomposition). The second one occurs above 370 °C, and is associated to the pyrolysis of the PCL fraction present in the mixtures.

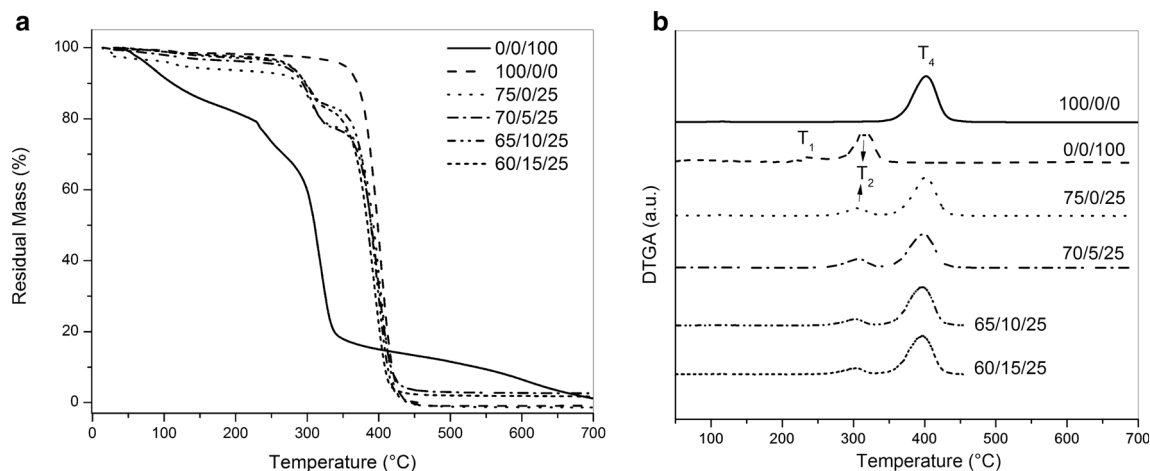


**Fig. 8** Thermogravimetric analysis of pure polymers and blends with 25 wt.% of TPS25 as a function of PCL-gAM content: **a** TGA; **b** DTGA

The temperatures for the maximum degradation rates of these events were called T<sub>2</sub> and T<sub>4</sub>, respectively. The temperature for TPS25 decomposition (T<sub>2</sub>) was not significantly modified by the presence of PCL nor PCL-gAM. In addition, the temperature for PCL decomposition (T<sub>4</sub>) was not significantly modified as a function of TPS content but was slightly suppressed as a function of PCL-gAM content, probably because the chemical modification with maleic anhydride reduces the molecular weight of PCL.

#### Chemical Structure (FTIR)

Figure 9 shows the FTIR spectra of the pure polymers and blends with 25 wt.% of TPS25 as a function of PCL-gAM content.

The characteristic peaks of PCL at 3000–2800, 1721, 850–1480 and 730 cm<sup>-1</sup> appeared in all specimens instead of pure TPS25. On the other hand, the FTIR spectra of PCL/TPS25 and PCL/PCL-gAM/TPS25 blends showed more intense peaks at 3200–3700 cm<sup>-1</sup> than that of the pure PCL spectra, which were assigned to O-H bond stretching vibration. This is because the OH group of TPS25 contributes to the bond stretching vibration [26].

The intensity of the peak centered at 3300 cm<sup>-1</sup>, corresponding to OH groups of starch, is suppressed in the spectra of the blends. This may be an evidence of reaction between the OH groups of starch and reactive groups present in PCL-gAM. The formation of hydrogen bonds between the hydroxyl groups of the carbonyl groups of TPS25 and PCL is one of the possible reactions [4]. Then the spectra of PCL/TPS blends are similar to those of pure PCL. The typical anhydride band at 1780 cm<sup>-1</sup> could not be observed because of overlapping of the intense PCL band at 1720 cm<sup>-1</sup> [12].

#### Morphology (SEM)

Figure 10(a-l) shows the SEM images of the PCL/TPS25 blends as a function of PCL-gAM content.

The holes in the micrographs represent the location of the TPS25 phase which was removed after the treatment with HCl. Holes size distribution could not be analyzed due to the irregular shape of the holes. Even so, it can be observed that the samples with 5 wt.% of PCL-gAM show the most regular sized, best distributed and smallest holes, independently on the TPS25 content. This may be a consequence of the optimization of PCL/TPS compatibility at this PCL-gAM concentration. Other authors have found optimal PCL/starch compatibilization adding 10 wt.% of pre-compatibilizer that consisted on PCL chemically modified with pyromellitic anhydride [12]. Increasing the PCL-gAM content above 5 wt.%, the hole distribution get worse and irregular shaped and bigger holes were observed, independently on the TPS25 content. On

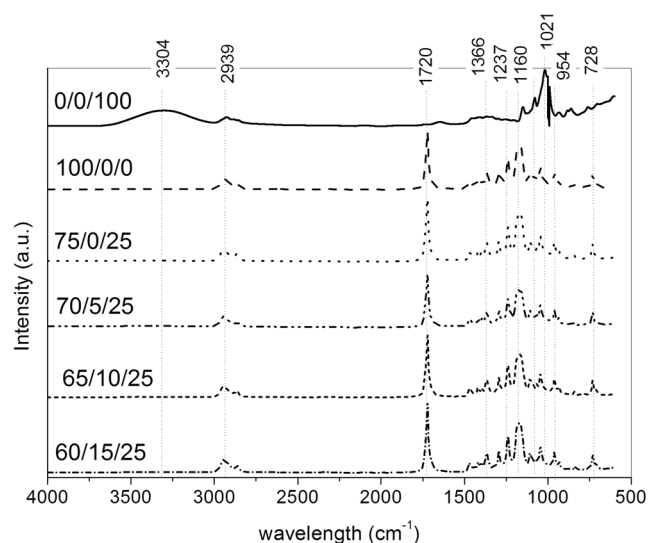


**Fig. 9** FTIR spectra of pure polymers and blends with 25 wt.% of TPS25 as a function of PCL-gAM content



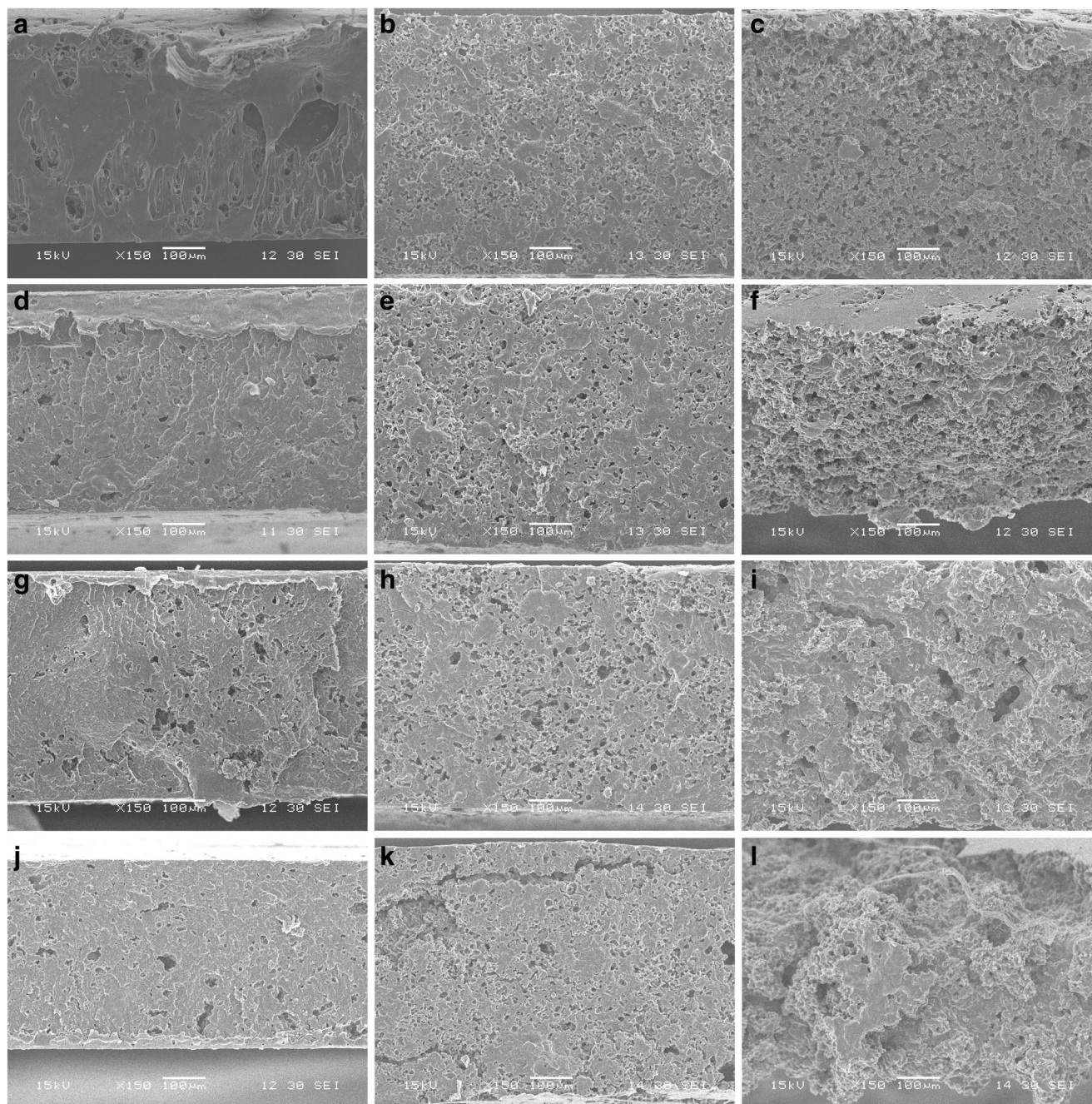


**Fig. 10** SEM images of the PCL/TPS25 samples as a function of PCL-gAM content: **a** 75/0/25; **b** 50/0/50; **c** 25/0/75; **d** 70/5/25; **e** 45/5/50; **f** 20/5/75; **g** 65/10/25; **h** 40/10/50; **i** 15/10/75; **j** 60/15/25; **k** 35/15/50; **l** 10/15/75

the other hand, increasing the amount of TPS25 increases the size and number of the TPS25 phase without modifying its distribution, independently on the PCL-gAM content analyzed.

#### *Mechanical Properties (Tensile Tests)*

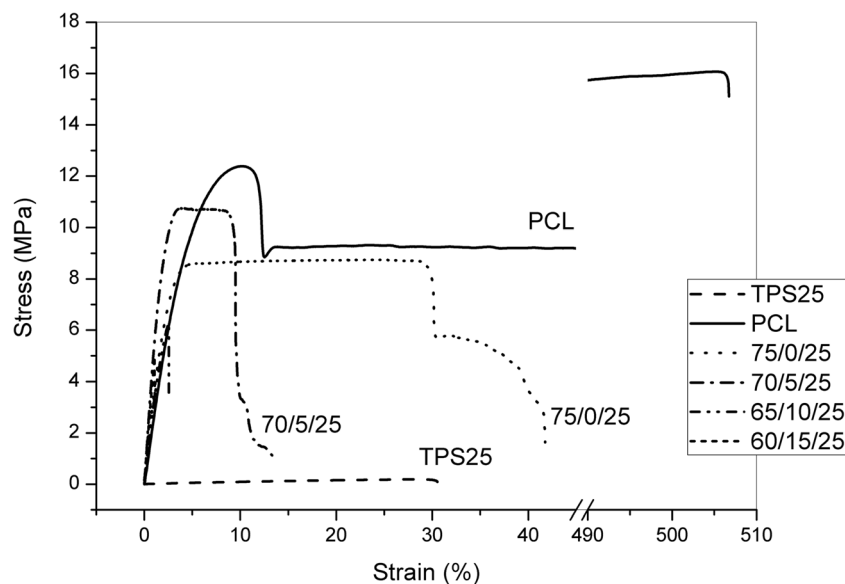
Figure 11 shows the stress strain curves of the pure polymers and blends with 25 wt.% of TPS25 as a function of PCL-gAM

content. Only blends with 25 wt.% of TPS25 were included for the sake of simplicity.

Mechanical properties such as Young's modulus ( $E$ ), maximum stress ( $\sigma$ ) and elongation at break ( $\epsilon$ ) were calculated from the stress-strain curves obtained in the tensile tests. The results are summarized in Table 4.

PCL is a ductile polymer, able to undergo large deformations; but unfortunately it shows a relatively low stiffness rendering it unable to be used for any applications where a high rigidity is required [7]. The presence of

**Fig. 11** Stress–strain curves of the pure polymers and blends with 25 wt.% of TPS25 as a function of PCL-gAM content



TPS25 in the blends do not contribute to increase the stiffness of the films, because pure TPS25 modulus is significantly lower than the modulus of pure PCL.

Concerning the Young's moduli of PCL/TPS25 blends containing PCL-gAM, higher values than the neat PCL and TPS25 polymers were observed. The mechanical properties of the compatibilizer (PCL-gAM) could not be calculated because the samples were so fragile that dog-bone specimens for mechanical testing could not be prepared. Even so, we noticed that the stiffness of the compatibilizer sheets was significantly higher than that of the sheets prepared with the neat PCL and TPS25 polymers. For this reason, the Young's moduli of the PCL/TPS25 blends containing

PCL-gAM are higher than that of the pure polymers. In addition, an optimal PCL-gAM content is observed at 5 wt.% for all TPS25 contents analyzed. This result is in accordance with the SEM analysis that confirmed the optimal compatibilization at this concentration. The increment in the Young's modulus is accompanied with a detriment in the elongation at break. This is a consequence of the improved distribution and lower size of the TPS25 phase that hinder the movement of the PCL phase chains [12].

#### Biodegradation in soil

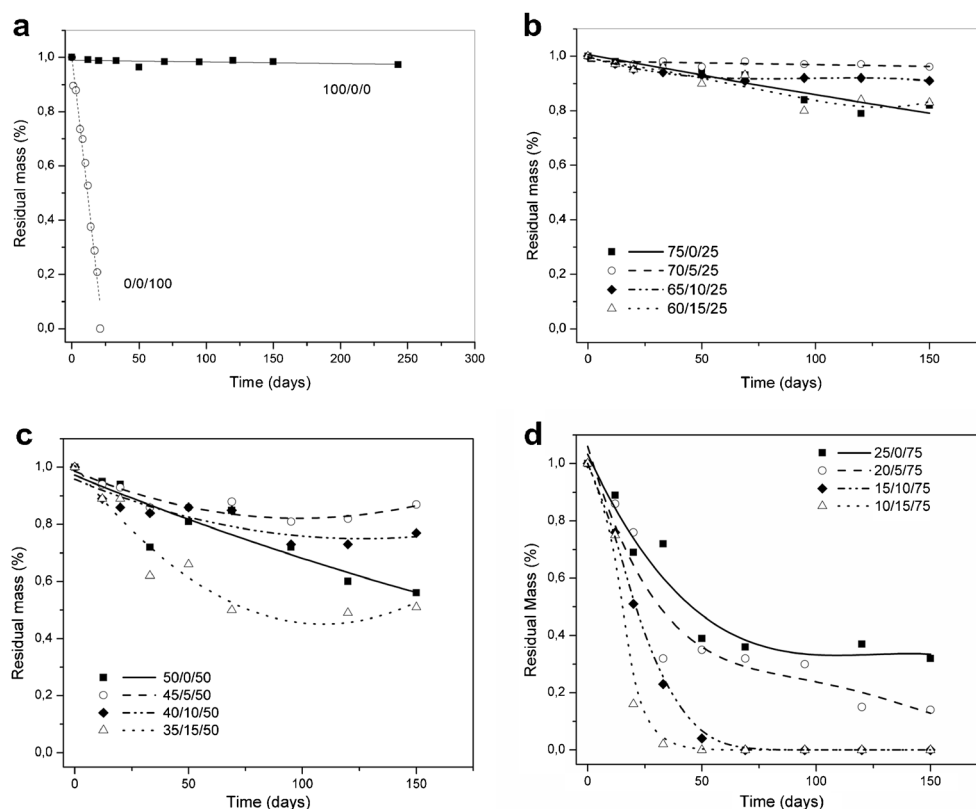
Figure 12(a–d) shows the curves of weight loss as a function of time for all materials after biodegradation in soil.

Figure 12(a) shows that the pure TPS25 is completely degraded after 21 days of burial in soil. On the other hand, only 1 % of the initial pure PCL mass was degraded after 21 days. In addition, only 3 % of the pure PCL was degraded after 243 days. In the case of the blends, the degradation rate increases as a function of the TPS25 content. In the soil, water diffused into the polymer sample, causing swelling and enhancing biodegradation, so it is expected higher degradation rate for the most hydrophilic sample [3]. In the case of the compatibilized samples, the blends containing 5 wt.% of PCL-gAM showed the slowest biodegradation rate independently of the TPS25 content. The enhanced PCL/TPS compatibility of the samples with 5 wt.% of PCL-gAM, which was shown by SEM and mechanical properties analysis, may be decreasing the water absorption capacity of TPS25 slowing down the biodegradation rate.

**Table 4** Mechanical properties of the pure polymers and blends

Sample	$E$ (MPa)	$\sigma$ (MPa)	$\epsilon$ (%)
100/0/0	425±4	17.4±2.1	477.4±41.5
75/0/25	178±2	9.4±0.3	52.0±8.0
70/5/25	545±7	11.6±0.5	25.6±10.1
65/10/25	349±23	6.0±0.2	2.0±0.3
60/15/25	539±16	4.6±0.5	1.2±0.2
50/0/50	142±18	16.0±1.3	6.0±0.4
45/5/50	681±9	5.7±0.4	4.0±1.0
40/10/50	588±11	5.0±0.6	2.6±0.5
35/15/50	692±11	7.5±0.2	1.2±0.0
25/0/75	243±2	2.6±0.2	3.6±0.3
20/5/75	1020±9	4.5±0.3	1.4±0.2
15/10/75	990±17	5.2±1.1	0.7±0.1
10/15/75	—	—	—
0/0/100	13±2	0.9±0.1	33±0.3





**Fig. 12** Residual mass as a function of time after biodegradation in soil of the **a** pure polymers and the blends with **b** 25 wt.%, **c** 50 wt.% and **d** 75 wt.% of TPS25 as a function of PCL-gAM content

## Conclusions

PCL/PCL-gAM/TPS blends were obtained by melt mixing and compression molding and their properties were investigated. The optimal plasticizer content in the synthesis of TPS was analyzed. The lowest water vapor absorption and the strongest mechanical properties were obtained using 25 wt.% of ethylene glycol. In the case of the blends, an optimal compatibilizer content was found. The highest Young's modulus was obtained with the blend containing 5 wt.% of compatibilizer (PCL-gAM), which was attributed to the enhanced compatibility between the pure PCL and the TPS25 phases demonstrated by SEM. In contrast, the water vapor absorption increased by the addition of the compatibilizer.

The thermal stability of TPS was not significantly modified by the presence of PCL nor PCL-gAM. On the other hand, the thermal stability of PCL was reduced the addition of PCL-gAM which may be a consequence of the reduction of the molecular weight of PCL after the chemical modification. On the other hand, the crystallinity degree of PCL slightly increased in the presence of TPS25. TPS25 could be acting as nucleation agent increasing the crystallization rate of the PCL phase. The glass transition temperature of PCL was slightly increased by the presence of PCL-gAM, which was

attributed to the reduced segmental motion of random coil chains in amorphous regions and increased free volume through the presence in the end- chain of the encumbering molecules of maleic anhydride.

Finally, it was observed that the degradation rate in soil on the blends increases as a function of the TPS25 content due to the hydrophilic nature of this component. In the case of the blends, the slowest degradation rate was obtained in the sample with 5 wt.% of compatibilizer, which was attributed to the enhanced compatibility between pure PCL and TPS25 phases.

**Acknowledgments** This work was supported by National Scientific and Technical Research Council (CONICET), the National Agency of Science and Technology (ANPCyT) [Fonarsc FSNano004], and the National University of Mar del Plata (UNMDP) [15G327].

## References

- Da Róz AL, Carvalho AJF, Gandini A, Curvelo AAS (2006) The effect of plasticizers on thermoplastic starch compositions obtained by melt processing. *Carbohydr Polym* 63:417–424
- Avérous L, Moro L, Dole P, Fringant C (2000) Properties of thermoplastic blends: starch-polycaprolactone. *Polymer (Guildf)* 41: 4157–4167

3. Wu C-S (2003) Physical properties and biodegradability of maleated-polycaprolactone/starch composite. *Polym Degrad Stab* 80:127–134. doi:[10.1016/S0141-3910\(02\)00393-2](https://doi.org/10.1016/S0141-3910(02)00393-2)
4. Chen L, Ni Y, Bian X et al (2005) A novel approach to grafting polymerization of  $\epsilon$ -caprolactone onto starch granules. *Carbohydr Polym* 60:103–109. doi:[10.1016/j.carbpol.2004.11.028](https://doi.org/10.1016/j.carbpol.2004.11.028)
5. Buléon A, Colonna P, Planchot V, Ball S (1998) Starch granules: structure and biosynthesis. *Int J Biol Macromol* 23:85–112. doi:[10.1016/S0141-8130\(98\)00040-3](https://doi.org/10.1016/S0141-8130(98)00040-3)
6. Matzinos P, Tserki V, Kontoyiannis A, Panayiotou C (2002) Processing and characterization of starch/polycaprolactone products. *Polym Degrad Stab* 77:17–24. doi:[10.1016/S0141-3910\(02\)00072-1](https://doi.org/10.1016/S0141-3910(02)00072-1)
7. Averous L, Moro L, Dole P, Fringant C (2000) Properties of thermoplastic blends: starch–polycaprolactone. *Polymer (Guildf)* 41:4157–4167. doi:[10.1016/S0032-3861\(99\)00636-9](https://doi.org/10.1016/S0032-3861(99)00636-9)
8. Bikiaris D, Prinos J, Koutsopoulos K et al (1998) LDPE/plasticized starch blends containing PE-g-MA copolymer as compatibilizer. *Polym Degrad Stab* 59:287–291. doi:[10.1016/S0141-3910\(97\)00126-2](https://doi.org/10.1016/S0141-3910(97)00126-2)
9. Reis KC, Pereira J, Smith AC et al (2008) Characterization of polyhydroxybutyrate-hydroxyvalerate (PHB-HV)/maize starch blend films. *J Food Eng* 89:361–369. doi:[10.1016/j.jfoodeng.2008.04.022](https://doi.org/10.1016/j.jfoodeng.2008.04.022)
10. Sarazin P, Li G, Orts WJ, Favis BD (2008) Binary and ternary blends of polylactide, polycaprolactone and thermoplastic starch. *Polymer (Guildf)* 49:599–609. doi:[10.1016/j.polymer.2007.11.029](https://doi.org/10.1016/j.polymer.2007.11.029)
11. Marrakchi Z, Oueslati H, Belgacem MN et al (2012) Biocomposites based on polycaprolactone reinforced with alfa fibre mats. *Compos Part A Appl Sci Manuf* 43:742–747. doi:[10.1016/j.compositesa.2011.12.027](https://doi.org/10.1016/j.compositesa.2011.12.027)
12. Avella M, Errico ME, Laurienzo P et al (2000) Preparation and characterisation of compatibilised polycaprolactone/starch composites. *Polymer (Guildf)* 41:3875–3881. doi:[10.1016/S0032-3861\(99\)00663-1](https://doi.org/10.1016/S0032-3861(99)00663-1)
13. John J, Tang J, Yang Z, Bhattacharya M (1997) Synthesis and characterization of anhydride-functional polycaprolactone. *J Polym Sci Part A Polym Chem* 35:1139–1148. doi:[10.1002/\(sici\)1099-0518\(19970430\)35:6<1139::aid-pola17>3.0.co;2-7](https://doi.org/10.1002/(sici)1099-0518(19970430)35:6<1139::aid-pola17>3.0.co;2-7)
14. Yam WY, Ismail J, Kammer HW et al (1999) Polymer blends of poly( $\epsilon$ -caprolactone) and poly(vinyl methyl ether) – thermal properties and morphology. *Polymer (Guildf)* 40:5545–5552. doi:[10.1016/S0032-3861\(98\)00807-6](https://doi.org/10.1016/S0032-3861(98)00807-6)
15. Lourdin D, Coignard L, Bizot H, Colonna P (1997) Influence of equilibrium relative humidity and plasticizer concentration on the water content and glass transition of starch materials. *Polymer (Guildf)* 38:5401–5406
16. Soares RMD, Lima AMF, Oliveira RVB et al (2005) Thermal degradation of biodegradable edible films based on xanthan and starches from different sources. *Polym Degrad Stab* 90:449–454. doi:[10.1016/j.polyimdegradstab.2005.04.007](https://doi.org/10.1016/j.polyimdegradstab.2005.04.007)
17. Canché-Escamilla G, Canché-Canché M, Duarte-Aranda S et al (2011) Mechanical properties and biodegradation of thermoplastic starches obtained from grafted starches with acrylics. *Carbohydr Polym* 86:1501–1508. doi:[10.1016/j.carbpol.2011.06.052](https://doi.org/10.1016/j.carbpol.2011.06.052)
18. Wilhelm HM, Sierakowski MR, Souza GP, Wypych F (2003) Starch films reinforced with mineral clay. *Carbohydr Polym* 52:101–110
19. Janković B (2013) Thermal characterization and detailed kinetic analysis of Cassava starch thermo-oxidative degradation. *Carbohydr Polym* 95:621–9. doi:[10.1016/j.carbpol.2013.03.038](https://doi.org/10.1016/j.carbpol.2013.03.038)
20. Guinesi LS, da Róz AL, Corradini E et al (2006) Kinetics of thermal degradation applied to starches from different botanical origins by non-isothermal procedures. *Thermochim Acta* 447:190–196. doi:[10.1016/j.tca.2006.06.002](https://doi.org/10.1016/j.tca.2006.06.002)
21. Prachayawarakorn J, Ruttanabus P, Boonsom P (2010) Effect of cotton fiber contents and lengths on properties of thermoplastic starch composites prepared from rice and waxy rice starches. *J Polym Environ* 19:274–282. doi:[10.1007/s10924-010-0273-1](https://doi.org/10.1007/s10924-010-0273-1)
22. Prachayawarakorn J, Chaiwatyothin S, Mueangta S, Hanchana A (2013) Effect of jute and kapok fibers on properties of thermoplastic cassava starch composites. *Mater Des* 47:309–315. doi:[10.1016/j.matdes.2012.12.012](https://doi.org/10.1016/j.matdes.2012.12.012)
23. Velasquez D, Pavon-Djavid G, Chaunier L et al (2015) Effect of crystallinity and plasticizer on mechanical properties and tissue integration of starch-based materials from two botanical origins. *Carbohydr Polym* 124:180–187. doi:[10.1016/j.carbpol.2015.02.006](https://doi.org/10.1016/j.carbpol.2015.02.006)
24. Valderrama Solano AC, Rojas de Gante C (2014) Development of biodegradable films based on blue corn flour with potential applications in food packaging. Effects of plasticizers on mechanical, thermal, and microstructural properties of flour films. *J Cereal Sci* 60:60–66. doi:[10.1016/j.jcs.2014.01.015](https://doi.org/10.1016/j.jcs.2014.01.015)
25. Jost V, Kobsik K, Schmid M, Noller K (2014) Influence of plasticiser on the barrier, mechanical and grease resistance properties of alginate cast films. *Carbohydr Polym* 110:309–19. doi:[10.1016/j.carbpol.2014.03.096](https://doi.org/10.1016/j.carbpol.2014.03.096)
26. Kalambur S, Rizvi SSH (2006) An overview of starch-based plastic blends from reactive extrusion. *J Plast Film Sheeting* 22:39–58